Journal of Engineering Mathematics **35:** 71–84, 1999.

On steady periodic interfacial waves

E. O. TUCK and L. H. WIRYANTO
Applied Mathematics Department, The University of Adelaide, Adelaide, 5005, Australia.
e-mail: etuck@maths.adelaide.edu.au

Received 31 August 1997; accepted in revised form 31 March 1998

Abstract. Periodic waves on the interface between a lower layer of heavy fluid and an upper light fluid extending to infinity are considered both exactly and in a shallow-layer approximation. The latter leads to a composite long-wave equation combining Korteweg–de Vries and Benjamin–Ono characteristics, which is consistent in order when the density of the upper fluid is much less than that of the shallow lower layer. Comparison is made between numerical results from the exact and approximate theories, and with the analytic results of the separate Korteweg–de Vries and Benjamin–Ono equations which are special cases.

Keywords: interfacial, Benjamin–Ono, water waves, numerical

1. Introduction

Consider a periodic wave of wavelength $\lambda = 2\pi/k$, with the wave number k, on the interface $y = \eta(x)$ between a layer $0 < y < \eta$ of fluid of constant density ρ_1 and an upper fluid in $y > \eta(x)$ of density $\rho_2 < \rho_1$. The flow is assumed to be steady, with a uniform stream of magnitude c at $y = +\infty$. This is as seen in a frame of reference moving with the wave, and hence c can also be interpreted as the wave speed in a frame of reference fixed with respect to a stationary fluid at infinity.

In the present article we shall define a reference depth h of the heavy layer as the average interface height over a wavelength, *i.e.* by

$$h = \frac{1}{\lambda}\int_0^{\lambda} \eta(x)\,\mathrm{d}x. \tag{1}$$

This is a somewhat arbitrary definition, and there are circumstances in which other choices of a reference depth h are more suitable. For example, the special case of a solitary wave is just the limit as $\lambda \to \infty$ or $k \to 0$, but in that case it is more convenient before letting $k \to 0$ to define h as the depth at the troughs of the periodic wave, in which case the limiting h is the layer depth at $x = \pm\infty$, with the whole solitary wave lying above $y = h$. We could also in some cases allow h to be the arithmetic mean of trough and crest heights, etc., but prefer the above-defined mean height. We define the wave height H as the trough-to-crest distance, and for some purposes consider all quantities to be parametrised by (among others) the parameters k, H, *e.g.* $c = c(k, H)$.

Linearised theory applies for sufficiently small H relative to all other length scales, and indicates a sinusoidal wave

$$\eta = h + \tfrac{1}{2}H\cos kx \tag{2}$$

with (see Benjamin [1])

$$c^2 = \frac{g}{k}\left[\frac{(\rho_1 - \rho_2)\sinh kh}{\rho_1 \cosh kh + \rho_2 \sinh kh}\right]. \tag{3}$$

This defines $c(k, 0)$. We are also interested in the first terms in the long-wave, *i.e.* small-k expansion of this expression, namely

$$\frac{c(k,0)}{c_0} = 1 - \frac{1}{2}\frac{\rho_2}{\rho_1}kh + \left[\frac{3}{8}\left(\frac{\rho_2}{\rho_1}\right)^2 - \frac{1}{6}\right]k^2h^2 + \ldots, \tag{4}$$

where

$$c_0 = \sqrt{g^* h} \tag{5}$$

defines the classical linearised long-wave speed, with

$$g^* = \left(1 - \frac{\rho_2}{\rho_1}\right)g \tag{6}$$

as reduced gravity.

Our task now is to generalise these results to nonzero H. We first do this exactly, constructing a numerical solution without further approximation. We then develop an approximate equation describing the long-wave small-height case where both kh and H/h are small.

It is appropriate to quote the final equation immediately. Namely, if $f(x) = \eta(x)/h - 1$ denotes the relative perturbation of the interface profile from its undisturbed plane $y = h$, then $f(x)$ satisfies the integro-differential equation

$$-2\left[\frac{c}{c_0} - 1\right]f(x) + \tfrac{3}{2}[f(x)]^2 + \tfrac{1}{3}h^2 f''(x) + \frac{\rho_2}{\rho_1}h\mathcal{H}f'(x) = \tfrac{3}{2}\overline{f^2}\,, \tag{7}$$

where

$$\mathcal{H}f'(x) = \frac{1}{\pi}\int_{-\infty}^{\infty}\frac{f'(\xi)}{\xi - x}\,\mathrm{d}\xi \tag{8}$$

is a Hilbert transform. The right-hand side of (7) is a normalisation constant, with $\overline{f^2}$ the mean square value of $f(x)$, all but the squared term on the left having zero mean.

The Korteweg–de Vries (KdV) equation [2] is that obtained from (7) by omitting the term in $\mathcal{H}f'(x)$, whereas the Benjamin–Ono (BO) equation ([2, 3]) is that obtained by omitting the term in $f''(x)$. These equations are often encountered in a once-differentiated form, where the constant on the right is eliminated, and also often in a time-dependent form for unsteady waves in a fixed frame of reference.

The KdV equation is normally considered to hold when there is no upper fluid at all, *i.e.* $\rho_2 = 0$, and demands that $H/h = O(kh)^2$. The BO equation is normally considered to hold when there is an upper fluid of finite density ρ_2, and demands $H/h = O(kh)$. The full Equation (7) with all four terms present on the left can be seen to hold formally when the density ratio is small, formally with $H/h = O(kh)^2$ and $\rho_2/\rho_1 = O(kh)$, but in any case is

a useful empirical interpolator (with respect to the density) between the two established KdV and BO approximations. It may be called the 'composite long-wave equation' (CLW).

There is already in the literature ([4, 5]) an 'intermediate long-wave equation' (ILW) which plays a similar interpolating role, but with respect to the depth rather than the density. That equation applies to the case where the extent of the upper fluid is 'finite', in the sense that its height is large compared to the (small) height of the lower layer and comparable to the wavelength. This equation is essentially the same as the BO equation, but with the Hilbert transform operator (8) replaced by a more general integro-differential operator. This operator reduces to the Hilbert transform as the upper height tends to infinity, so recovering the BO equation. On the other hand, it yields essentially a two-fluid version of the KdV equation ([6, 7]) in the limit as the upper height reduces to a value comparable to the lower height, so that the whole fluid domain is then shallow.

In order to provide a benchmark against which to test the approximate KdV, CLW and BO theories, we must compute 'exact' solutions numerically. There have been many such numerical computations for free-surface waves, but few interfacial waves. Rienecker and Fenton [8] developed a method to calculate free-surface waves based on a truncated Fourier series. A closed system of equations is obtained by specifying two quantities defining the wave, such as wave height and period, so that the solution can then be obtained by the application of Newton's method to a system of discretised algebraic equations. This Fourier approximation is valid both for deep and shallow water, in which the wave is periodic. This method is further developed to calculate interface periodic waves in the present paper. Many other methods are available such as that given by Scullen and Tuck [9] who apply isolated sources located outside the flow domain to present the velocity potential in a series form. Vanden–Broeck and Schwartz [10] used an integral equation method to calculate steep gravity waves in shallow water. In earlier numerical work, extensions of Stokes's [11] series expansion method were used by Schwartz [12], Cokelet [13] and Longuet–Higgins [14] in infinite depth of water.

Numerical computations for waves on the interface between two unbounded fluids of different density can be found in papers by Holyer [15] and Saffman and Yuen [16] who presented the velocity potential of both fluids and the interface as Fourier series. Meanwhile, Vanden-Broeck [17] formulated the problem as a nonlinear integro-differential equation for the unknown shape of the interface.

The performance of most numerical methods for solving exact nonlinear waves deteriorates as the wave gets steeper, and these methods usually fail before we reach the highest possible wave. It is therefore an especially challenging task to compute these highest waves. For free-surface waves, Stokes [11] deduced that the wave would have a stagnation point at 120^0 crest for free-surface problems. Stokes formulated the problem as a perturbation expansion and obtained the solution to third order for waves on an infinitely deep fluid. This expansion was extended by Schwartz [12] and Cokelet [13] to determine the highest wave for various values of the water depth. Alternatively, Michell [18], in calculating the highest Stokes waves, developed a series solution for the complex velocity in terms of the complex potential. For interfacial waves, Stokes's 120^0 crest behaviour cannot occur, since this would imply infinite velocity in the fluid above the crest. As an alternative highest-wave criterion, Holyer [15] suggested that waves are limited by the occurrance of a vertical tangent in the interface. This criterion was not supported by Saffman and Yuen's conjecture [16], *i.e.* the waves exist until the interface intersects itself. In our calculation, the computer program fails to converge when attempting calculations at high wave amplitudes before satisfying Holyer's criterion. Further work is needed on this matter.

2. Exact equations and solution procedure

Assuming irrotational flow of an inviscid incompressible fluid in each separate region, we must solve Laplace's equation

$$\nabla^2\phi_1 = \nabla^2\phi_2 = 0 \tag{9}$$

for the separate velocity potentials $\phi_1(x, y)$ in $0 < y < \eta(x)$ and $\phi_2(x, y)$ in $y > \eta(x)$. The bottom condition is

$$\frac{\partial\phi_1}{\partial y} = 0 \quad \text{on } y = 0 \tag{10}$$

and the condition at infinity is

$$\phi_2 \to cx \quad \text{as } y \to \infty\,. \tag{11}$$

The two potentials ϕ_1, ϕ_2 are matched across the interface $y = \eta$, which is a stream surface, so both normal derivatives vanish, *i.e.*

$$\frac{\partial\phi_1}{\partial y} - \eta'(x)\frac{\partial\phi_1}{\partial x} = 0 \tag{12}$$

and

$$\frac{\partial\phi_2}{\partial y} - \eta'(x)\frac{\partial\phi_2}{\partial x} = 0 \tag{13}$$

on $y = \eta(x)$. Finally, we observe that the pressure is continuous across the interface, so that (using Bernoulli's equation)

$$-\rho_1\left[\tfrac{1}{2}\phi_{1x}^2 + \tfrac{1}{2}\phi_{1y}^2 + g\eta\right] + \rho_2\left[\tfrac{1}{2}\phi_{2x}^2 + \tfrac{1}{2}\phi_{2y}^2 + g\eta\right] = P = \text{constant}. \tag{14}$$

The value of the pressure constant P in (14) is one of the parameters ultimately determining the form of the wave.

In order to develop an exact numerical solution to this problem, it is somewhat more convenient to use the stream function ψ, the harmonic conjugate to ϕ. Then suitable solutions of Laplace's equation can be represented as series

$$\psi_1(x, y) = cy + \sum_{j=1}^{\infty} b_{1j}\sinh(jky)\ \cos(jkx) \tag{15}$$

and

$$\psi_2(x, y) = cy + \sum_{j=1}^{\infty} b_{2j}\exp(-jky)\ \cos(jkx). \tag{16}$$

The coefficients b_{1j} and b_{2j}, $j = 1, 2, \ldots$, are constants to be determined. These representations satisfy conjugates to (10) and (11).

To determine the interface profile $y = \eta(x)$ and the speed c, the series are truncated after the term with $j = N$ and substituted in the kinematic and dynamic conditions (12), (13) and (14). In terms of ψ_1 and ψ_2, these boundary conditions can be written as

$$\psi_1(x, \eta) = q_1, \tag{17}$$

$$\psi_2(x, \eta) = q_2, \tag{18}$$

and

$$\frac{1}{2}\left[(\psi_{1x}^2 + \psi_{1y}^2) - \frac{\rho_2}{\rho_1}(\psi_{2x}^2 + \psi_{2y}^2)\right] + g^*\eta = p_1, \tag{19}$$

where q_1, q_2 and $p_1 = -P/\rho_1$ are unknown constants. Finally, the interface is discretised, becoming $N + 1$ points with coordinate $(x_0, \eta_0), \ldots, (x_N, \eta_N)$ on a half-wavelength interval, where $x_0 = 0$ is located at a crest, and $x_N = \lambda/2$ at a trough.

The above discretisation gives $N + 1$ equations for each of the three boundary conditions, but the resulting system is not yet closed, since there are a total of $3N + 5$ unknowns, namely

$$\{b_{1j}, b_{2j};\ j = 1, \ldots N\}, \{\eta_j;\ j = 0, \ldots N\}, c, q_1, q_2, p_1.$$

Two further equations are therefore required. These equations are obtained from the prescribed characteristics of the wave, *i.e.* the wave height H and the average interface height h. Hence, the extra two equations are $H = \eta_0 - \eta_N$ and (1), in which the integral can be evaluated by the trapezoidal method. In practice, we nondimensionalize with λ set to 2π. We now have $3N + 5$ equations in $3N + 5$ unknowns, which are solved by standard methods. Results are presented later.

3. Composite long-wave approximation

We now assume that the interface is a small perturbation of the uniform plane $y = h$. Since that plane is itself a small departure from the bottom surface $y = 0$, it is important that the small dimensionless parameter which measures the wave height is taken as H/h, *i.e.* wave height relative to lower fluid depth. Meanwhile the appropriate nondimensional measure of smallness of h itself is kh, which is proportional to the depth to wavelength ratio. These two small parameters kh and H/h are in principle independent, but there are certain special relationships between them, in which the final approximate equations retain consistency. However, we now derive approximations to the exact equations without specifying any such a relationship.

Thus, in the following derivation, we retain leading-order terms in powers of kh and H/h. The errors in each equation are not explicitly stated, but in every case are at least one power of either of these parameters smaller than the orders of any retained term. Where the equations contain a 'constant', the order of magnitude of this constant is not specified, but is left to be determined by the final equation.

For small H/h, it is clear that the upper region flow is a small perturbation of the uniform stream $\phi_2 = cx$, which we write

$$\phi_2 = cx + \Phi_2 \tag{20}$$

for some perturbation potential Φ_2. The latter satisfies a linearised version of the boundary condition (13), namely

$$\frac{\partial \Phi_2}{\partial y} = c\eta'(x) \tag{21}$$

on the limiting plane $y = h$. Hence, as in thin airfoil theory (Newman, [19]), the solution in $y > h$ is

$$\Phi_2(x, y) = \frac{1}{\pi} \int_{-\infty}^{\infty} c\eta'(\xi)\ \log \sqrt{(x-\xi)^2 + (y-h)^2}\ \mathrm{d}\xi \tag{22}$$

from which follows immediately the perturbation x-wise velocity on the top side of the interface to leading order as

$$\Phi_{2x}(x, h) = -c\mathcal{H}\eta'(x)\ , \tag{23}$$

where $\mathcal{H}$ is the Hilbert transform defined in (8).

The connection between upper and lower regions is now entirely via the pressure continuity condition, which reduces to

$$-\rho_1 \left[\tfrac{1}{2}\phi_{1x}^2 + \tfrac{1}{2}\phi_{1y}^2 + g\eta\right] + \rho_2 \left[c\Phi_{2x} + g\eta\right] = \text{constant}$$

or

$$\tfrac{1}{2}\phi_{1x}^2 + \tfrac{1}{2}\phi_{1y}^2 + g^*\eta + \frac{\rho_2}{\rho_1}c^2\mathcal{H}\eta'(x) = \text{constant} \tag{24}$$

where g^* is as defined in (6).

The flow in the lower layer is strongly dependent on kh, and in that region we concentrate first on a small-depth expansion. This is of the form of a truncated Taylor series in y, *i.e.*

$$\phi_1(x, y) = \Phi_1(x) - \tfrac{1}{2}y^2\Phi_1''(x) + \tfrac{1}{24}y^4\Phi_1''''(x) \tag{25}$$

which automatically satisfies the Laplace equation and the bottom condition for any Φ_1. We write $u(x) = \Phi_1'(x)$. Substitution in the kinematic condition (12) on the interface yields

$$-\eta u' + \tfrac{1}{6}\eta^3 u''' = \eta' \left[u - \tfrac{1}{2}\eta^2 u''\right]$$

from which follows the one-dimensional continuity equation

$$\eta u - \tfrac{1}{6}\eta^3 u'' = \text{constant}. \tag{26}$$

A similar substitution in the pressure continuity equation (24) yields

$$\tfrac{1}{2}u^2 + \tfrac{1}{2}\eta^2(u'^2 - uu'') + g^*\eta + \frac{\rho_2}{\rho_1}c^2\mathcal{H}\eta'(x) = \text{constant}. \tag{27}$$

We are now in a position to further expand the lower-region flow with respect to H/h. In contrast to the upper-region expansion, it is necessary to carry terms of at least second order

in wave height. Thus we write $u = c + u_1 + u_2$ and $\eta = h + \eta_1 + \eta_2$ where subscripts denote orders with respect to H/h. Now (26) gives

$$\left[hu_1 + c\eta_1\right] + \left[hu_2 + c\eta_2 + u_1\eta_1\right] - \tfrac{1}{6}h^3u_1'' = \text{constant}. \tag{28}$$

Similarly, (27) gives

$$\left[cu_1 + g^*\eta_1\right] + \left[cu_2 + g^*\eta_2 + \tfrac{1}{2}u_1^2\right] - \tfrac{1}{2}h^2cu_1'' + \frac{\rho_2}{\rho_1}c^2\mathcal{H}\eta' = \text{constant}. \tag{29}$$

If we keep only the leading terms in (28), (29), these equations are consistent only if $c = c_0$, confirming the linearised long-wave result. Hence, in general $c = c_0 + c_1 + \ldots$, where c_1 is the first wave-height-dependent correction to the wave speed. At the same time, to leading order, (28) gives the relationship

$$u_1 = -\frac{c_0}{h}\eta_1 \tag{30}$$

between fluid velocity and wave elevation, by which u_1 can be eliminated from (28) and (29).

Using $c = c_0 + c_1$ in the first terms and replacing c by c_0 in all but the first terms of (28) and (29), and subtracting (28)/h from (29)/c_0 we also eliminate u_2, η_2, giving a single equation for $\eta_1(x)$, namely

$$-2\frac{c_1}{c_0}\frac{\eta_1}{h} + \frac{3}{2}\left(\frac{\eta_1}{h}\right)^2 + \tfrac{1}{3}h^2\left(\frac{\eta_1}{h}\right)'' + \frac{\rho_2}{\rho_1}h\mathcal{H}\left(\frac{\eta_1}{h}\right)' = \text{constant} \tag{31}$$

which is (7), when the constant on the right is determined by integrating both sides over a wavelength.

Equation (31) is consistent in order with all terms retained and all of $O(kh)^4$, if $H/h = O(kh)^2$ and $\rho_2/\rho_1 = O(kh)$. It is reduced to the KdV equation if $\rho_2 = 0$, or indeed whenever ρ_2/ρ_1 is of smaller order than $O(kh)$. On the other hand, the BO equation is the approximation that arises with the second derivative term omitted and all remaining terms of $O(kh)^2$, if $H/h = O(kh)$ and $\rho_2/\rho_1 = O(1)$.

4. KdV and BO analytic solutions

4.1. KdV SOLUTION

In the case where there is no upper fluid ($\rho_2 = 0$), the approximate equation is of KdV type. The periodic solution is a cnoidal function, namely

$$f(x) = a + b\,\mathrm{cn}^2(x/m), \quad b = \tfrac{4}{3}h^2m, \quad a = -\frac{b}{K}\left[\frac{E - (1-m)K}{m}\right],$$

where K is a complete elliptic integral

$$K = \int_0^{\pi/2} \frac{\mathrm{d}\theta}{\sqrt{1 - m\,\sin^2\theta}},$$

and E is the complete elliptic integral of the second kind,

$$E = \int_0^{\pi/2} \sqrt{1 - m\,\sin^2\theta}\,\mathrm{d}\theta.$$

The parameter m determines the wavelength, and $0 < m < 1$ with $m = 0$ for cosine waves and $m \to 1$ for solitary ones. Moreover, the wave speed can be related to the parameter a, that is

$$c/c_0 = 1 + \tfrac{3}{2}a - \tfrac{2}{3}h^2(1 - 2m).$$

4.2. BO SOLUTION

In the case where the second derivative term in the CLW equation (7) is omitted, giving the BO equation, we summarise the analytic solution as given by Benjamin [1], namely

$$f(x) = \tfrac{2}{3}R\left[\frac{1-\beta^2}{1+\beta^2+2\beta\cos kx} - 1\right]$$

with

$$c/c_0 = 1 + R\left[\frac{1}{2}\left(\frac{1+\beta^2}{1-\beta^2}\right) - 1\right],$$

where

$$R = \frac{\rho_2}{\rho_1}kh.$$

Hence, the wave height can be represented as

$$H/h = \frac{8}{3}R\frac{\beta}{1-\beta^2}.$$

If this is used to eliminate β in c/c_0, we obtain

$$c/c_0 = 1 - R + \sqrt{\frac{1}{4}R^2 + \frac{9}{64}\left(\frac{H}{h}\right)^2}.$$

Here β is an input parameter ultimately determining the wave height, and $0 < \beta < 1$, with $\beta \approx 0$ for infinitesimal waves, and $\beta \to 1$ for waves of maximum height.

5. Numerical results

The exact numerical procedure developed in Section 2 is used to compute the interfacial profile $y = \eta(x)$ and the speed c, for various values of the three given non-dimensional parameters ρ_2/ρ_1, kh and H/h. The speed is presented in the form of the ratio c/c_0 for scaling purposes, so that it can be plotted versus H/h on the same plane for various ρ_2/ρ_1. The closed system of Equations (15) and (16) is solved by the NAG routine IC05NBF and the integral in (1) is calculated by ID01GAF. Accuracy for c/c_0 of at least 5 decimals is achieved for $N \geqslant 25$.

Most of the calculations are performed with $N = 30$. As the initial guess, a simple cosine profile is used where the stream functions (15) and (16) contain only two non-zero terms.

The approximate CLW equation for the scaled interfacial wave elevation $f(x)$ is (7), which also reduces in special cases to either the KdV or BO equation. The analytic solution of these special equations is given in the previous section, and is such that η and c/c_0 can be calculated explicitly after balancing the characteristics of the wave. The full CLW approximate equation does not appear to have such an analytic solution, and must itself be solved numerically. This can be done by a truncated cosine Fourier series

$$f(x) = \sum_{j=1}^{N} a_j \cos(j\,x), \tag{32}$$

for (7), since $\bar{f} = 0$ and f is assumed an even function. The procedure is similar to that used for the exact problem, *i.e.* we determine a_j $(j = 1, 2, \ldots, N)$, c/c_0 and δ denoting the right-hand side of (7). We can check the result by comparing δ with the value $\frac{3}{2}\overline{f^2}$ calculated from the mean square value of the series (32), and accurate agreement is achieved to at least 5 decimals. This numerical method can also be used to recalculate KdV and BO solutions, where the result is also in good agreement with the analytic solutions.

In discussing the results, we present wave speeds and profiles in different subsections. We illustrate the profiles only in a half-wavelength interval $[0, \pi/2]$.

5.1. WAVE SPEEDS

The results for c/c_0 (exact and approximations) are discussed below in two cases, namely for $H/h = 0$ (corresponding to linearised theory), and for $H/h \neq 0$, based on our numerical results. The wave speeds are first calculated at the typical value $kh = 0{\cdot}1$, for various ρ_2/ρ_1. Then, these calculations are repeated for $kh = 0{\cdot}2$ to observe the effect of this parameter.

We first consider the relation (4) from the linear theory. The approximations of (4) corresponding to the approximate equations are

$$\text{CLW}: \quad \frac{c(k,0)}{c_0} = 1 - \frac{1}{2}\frac{\rho_2}{\rho_1}kh - \tfrac{1}{6}k^2h^2, \tag{33}$$

$$\text{KdV}: \quad \frac{c(k,0)}{c_0} = 1 - \tfrac{1}{6}k^2h^2, \tag{34}$$

$$\text{BO} \;: \quad \frac{c(k,0)}{c_0} = 1 - \frac{1}{2}\frac{\rho_2}{\rho_1}kh. \tag{35}$$

The relation (34) is the limiting case of (33) with $\rho_2/\rho_1 \to 0$. Hence, we focus our description below only on (33) and (35).

In comparing (4) to (33) and (35), we note that the dispersion relation (33) has a truncation error $3(\rho_2/\rho_1)^2(kh)^2/8$. This error is less than the third term of (4), which is the truncating error of the BO dispersion relation (35), when $\rho_2/\rho_1 < 0.471$ for any value kh. Therefore, the CLW equation is the appropriate approximation in that interval for the problem here. In contrast, (35) gives smaller error for $\rho_2/\rho_1 > 0{\cdot}471$, and the third term of (4) reaches zero at $\rho_2/\rho_1 = 2/3$.

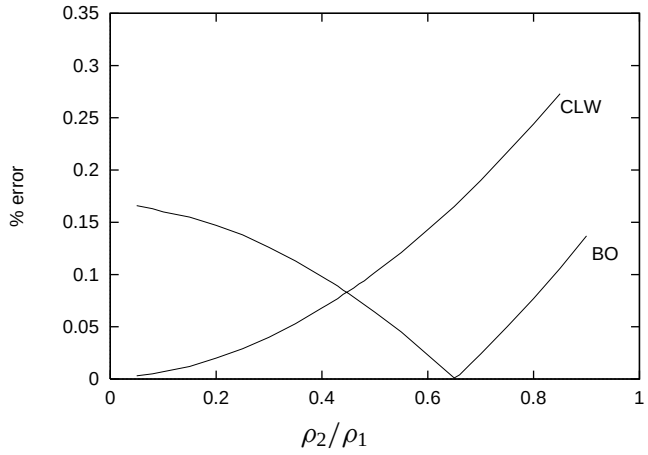

Figure 1. Plot of the percentage error versus ρ_2/ρ_1 at $kh = 0{\cdot}1$, $H/h = 0{\cdot}01$.

Now, we define the percentage error of c/c_0 for $H/h \neq 0$ from the CLW and BO equations with respect to the exact wave-speed, namely

$$e_{\mathrm{CLW}} = |c/c_0(\text{exact}) - c/c_0(\text{CLW})|\, 100\%, \tag{36}$$

$$e_{\mathrm{BO}} = |c/c_0(\text{exact}) - c/c_0(\text{BO})|\, 100\%. \tag{37}$$

A plot of e_{CLW} and e_{BO} versus ρ_2/ρ_1 is shown in Figure 1 for $kh = 0{\cdot}1$ and $H/h = 0{\cdot}01$. For small values of ρ_2/ρ_1, the CLW equation gives a good agreement to the exact result. We found that 0·02% error is reached at $\rho_2/\rho_1 = 0{\cdot}2$, and this error increases on increasing ρ_2/ρ_1. Meanwhile, the BO equation gives 0.147% error at the same value $\rho_2/\rho_1 = 0{\cdot}2$. The curve of the BO error reaches a minimum value at $\rho_2/\rho_1 = 0{\cdot}652$, and then increases again. The pattern of those curves confirms the result described above from the linear theory. The intersection point here corresponds to the critical value of ρ_2/ρ_1 where the CLW and BO equations give the same error. We found that this intersection point is at $\rho_2/\rho_1 = 0{\cdot}445$ with 0·084% error.

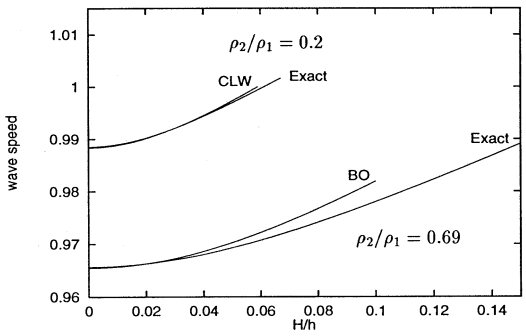

Figure 2. Plot of wave speed c/c_0 versus H/h at $kh = 0{\cdot}1$.

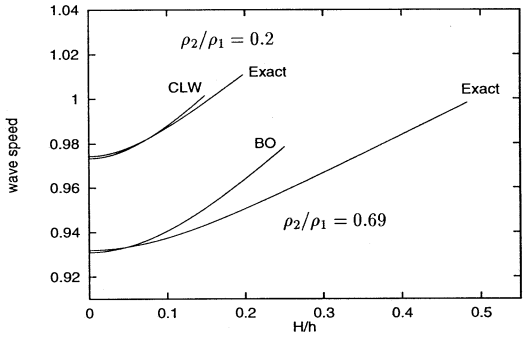

Figure 3. Plot of wave speed c/c_0 versus H/h at $kh = 0{\cdot}2$.

In describing our results for various H/h, we show a plot of c/c_0 versus H/h in Figure 2 for $\rho_2/\rho_1 = 0{\cdot}2$ and 0·69 at the heavy-fluid depth $kh = 0{\cdot}1$. The choice of these two values of ρ_2/ρ_1 is based on the percentage error computed above, where the BO approximation is less accurate than the CLW approximation at $\rho_2/\rho_1 = 0{\cdot}2$ and the other way around for $\rho_2/\rho_1 = 0{\cdot}69$. Therefore, we compare the exact wave-speed only with one of those approximations for

each value ρ_2/ρ_1 given above. The maximum values of H/h that can be used to calculate c/c_0 exactly by our numerical procedure are $H/h = 0{\cdot}068$ for $\rho_2/\rho_1 = 0{\cdot}2$ and $H/h = 0{\cdot}181$ for $\rho_2/\rho_1 = 0{\cdot}69$ but in Figure 2, we give results only up to $H/h = 0{\cdot}15$. The curve of the exact wave-speed for $\rho_2/\rho_1 = 0{\cdot}2$ is accompanied with the result from the CLW equation, and the exact curve for $\rho_2/\rho_1 = 0{\cdot}69$ is shown together with the result from the BO equation. If we tolerate 0·02% error from the exact speed, our computations give the maximum CLW wave-height $H/h = 0{\cdot}058$ for $\rho_2/\rho_1 = 0{\cdot}2$ and the maximum BO wave-height $H/h = 0{\cdot}028$ for $\rho_2/\rho_1 = 0{\cdot}69$.

All we have explained in the above are typical calculations for the shallow depth $kh = 0{\cdot}1$. Another less-shallow nondimensional reference depth, $kh = 0{\cdot}2$, is used to repeat the previous discussion, so that we can observe the effect of this depth parameter in decreasing the accuracy of the shallow-water approximate theory. The result is shown as a plot of c/c_0 versus H/h in Figure 3. We can compare this figure to Figure 2. At small values of H/h, the plot shows a difference between exact and approximate speeds, *i.e.* for bigger kh the difference is also bigger. As an illustration, we obtained $e_{\mathrm{CLW}} = e_{\mathrm{BO}} = 0{\cdot}02\%$ in Figure 2, and $e_{\mathrm{CLW}} = 0{\cdot}104\%$, $e_{\mathrm{BO}} = 0{\cdot}098\%$ in Figure 3 at the same value $H/h = 0{\cdot}01$. This agrees with the result at $H/h = 0$ from the linear theory where the truncation error from (4) is of order $(kh)^3$.

5.2. PROFILES

As we can see in Figure 2, $H/h = 0{\cdot}06$ is a relatively high wave, but still one where the exact numerical procedure converges for all ρ_2/ρ_1. This value of H/h is used to test the character of the interfacial profile. We first observe the variation of the exact profile for various ρ_2/ρ_1. A sharp-crested wave with a flat trough is the characteristic of small ρ_2/ρ_1. For larger values of ρ_2/ρ_1 (at the same value $H/h = 0{\cdot}06$), the point $x = x_{1/2}$ corresponding to the mid-level between the crest and the trough, shifts to the right and is followed by decreasing $\eta(x_{1/2})$ towards kh, so that the profile becomes more symmetric between crest and trough, and approaches a cosine form as $\rho_2/\rho_1 \to 1$.

The difference between exact and approximate profiles is affected by changing ρ_2/ρ_1. Sharp-crested approximate waves (BO and CLW) are also obtained for small ρ_2/ρ_1, but the BO equation produces unreasonably sharper crests, which are very much different from the exact profile, *i.e.* they have much smaller $x_{1/2}$ and much higher η_{crest} and η_{trough} than the xact profiles. If we increase ρ_2/ρ_1, this error in the BO approximation becomes less significant. However, the CLW profile is still closer to the exact profile, and remains as accurate at finite ρ_2/ρ_1 as it was for small ρ_2/ρ_1. This can be seen in Figures 4 and 5, which show the BO, CLW and exact profiles for two different values of ρ_2/ρ_1, *i.e.* $\rho_2/\rho_1 = 0{\cdot}2$ and 0·69, respectively. The CLW and exact profiles in both figures are indistinguishable.

We now present the effect of varying wave height by considering the variation of the exact profile for $\rho_2/\rho_1 = 0{\cdot}2$ and various H/h, following the curve in Figure 2. The profiles are plotted together in Figure 6 for $H/h = 0{\cdot}05, 0{\cdot}06$ and $0{\cdot}067$. One feature of this plot is the point $x = x_{1/2}$ for each profile. The tangent of the profile at around this point becomes steeper with increasing amplitude, since the crest moves up and the trough moves in the opposite direction, but not at the same rate, *i.e.* the crest rises more than the trough falls. Hence, the profile is sharper for higher H/h. In Figure 7 similar profiles are shown for $\rho_2/\rho_1 = 0{\cdot}69$,

and $H/h = 0{\cdot}06$, $0{\cdot}12$ and $0{\cdot}18$. However, the highest wave-height that we can use does not give a vertical point as suggested by Holyer [15].

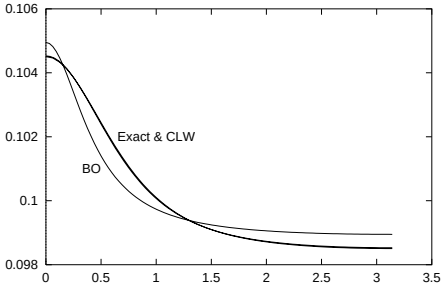

Figure 4. The interfacial profiles from the exact procedure and the approximate equations at $\rho_2/\rho_1 = 0{\cdot}2$, $kh = 0{\cdot}1$.

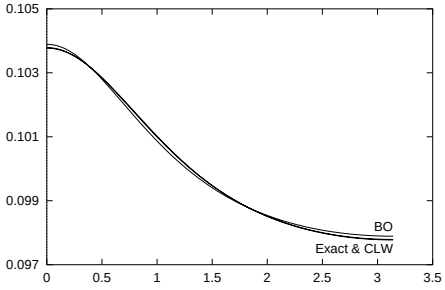

Figure 5. Similar to Figure 4, with $\rho_2/\rho_1 = 0{\cdot}69$.

The profile of the interface at $kh = 0{\cdot}2$ does differ significantly from calculations at $kh = 0{\cdot}1$ if we use the same value of H/h. However, the main difference is in the physical character, *i.e.* a larger wave height must be applied to get the same value of H/h for larger kh, which increases the level of the interface.

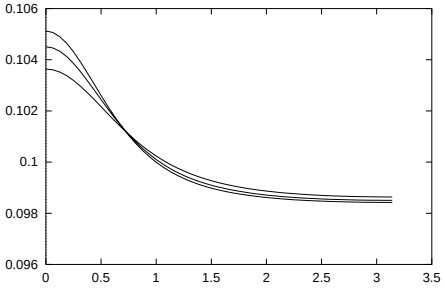

Figure 6. Three exact interfacial-profiles at $\rho_2/\rho_1 = 0{\cdot}2$, $kh = 0{\cdot}1$ and for $H/h = 0{\cdot}05$, $0{\cdot}06$, $0{\cdot}067$.

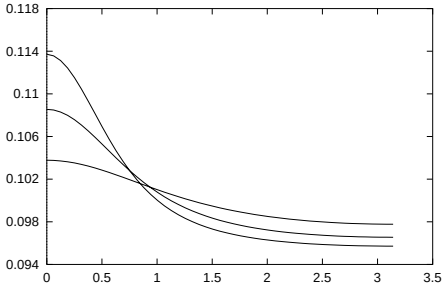

Figure 7. Three exact interfacial-profiles at $\rho_2/\rho_1 = 0{\cdot}69$, $kh = 0{\cdot}1$ and for $H/h = 0{\cdot}06$, $0{\cdot}12$, $0{\cdot}18$.

6. Concluding remarks

We have generalised the long-wave theories for one homogeneous layer (KdV) and for interfacial waves of a two-layer fluid with almost equal densities (BO). Our single equation representing the relative perturbation f of the interfacial profile from its undisturbed plane $y = h$ is given as equation (7) which is called the composite long-wave (CLW) equation. We found that the range of validity for the CLW equation is

$$\rho_2/\rho_1 = O(kh), \qquad H/h = O(kh)^2.$$

In describing the wave speed and profile of the interfacial waves, we used numerical methods to solve the CLW equation and to solve the 'exact' problem. Comparison was then made between both numerical results, and also with the analytic results of the BO equation. The

effect of each parameter (the density ratio, the wave height and the depth of the lower fluid) was observed on the speed and the profile of these interfacial waves.

Our exact calculations show that the wave speed increases monotonically with the wave height. Therefore, the highest wave is the fastest. For infinitesimal wave height, the speed agrees with the linearised theory. When the effect of the density ratio is included, an increase of the wave speed occurs with decreasing density ratio, where the smallest density ratio corresponds to free surface waves. The third parameter, the depth of the lower fluid, also has a reciprocal effect on the wave speed. Hence, an interfacial wave on a shallow lower-water is faster than a corresponding wave on a deep lower-water. This agrees with results in references on the free-surface problem (see [13] and [12]).

Moreover, we have also displayed the character of the nonlinear wave profile, where a sharp crest and a flat trough are the typical profile for small density ratio, and for large density ratio with large wave height. At a fixed wave height, this must change smoothly to a different form as the density ratio increases, *i.e.* a larger density ratio gives less nonlinearity, and hence a more nearly cosine profile, which is more symmetric between the crest and the trough. The nonlinearity from small density ratio can be preserved for larger density ratio by increasing the wave height. Note that our exact procedure is able to compute high waves accurately, but the highest solution with a vertical portion of the interface could not be reached.

In general, the above conclusions can be shown both from the exact calculations and the two approximate equations, *i.e.* the BO and the CLW equations. The KdV equation is just a special case of the CLW equation corresponding to zero density ratio. This shows that the approximations give the same qualitative result. Quantitatively, they are also both in good agreement with the exact computations for small wave amplitude and a finite (non-small) density ratio. However, the CLW equation is a significant improvement over the BO equation for small density ratio.

Acknowledgements

The second author is a staff member of the Department of Mathematics, Bandung Institute of Technology, Ganesha street 10, Bandung, Indonesia. This research was done when he was a PhD student at the University of Adelaide supported by Australian Agency for International Development (Ausaid).

References

1. T. B. Benjamin, Internal waves of permanent form in fluids of great depth. *J. Fluid Mech.* 29 (1967) 559–599.
2. D. J. Korteweg and G. de Vries, 1895, On the change of form of long waves advancing in a rectangular canal, and on a new type of long stationary waves. *Philos. Mag.* 39 (1895) 422–443.
3. H. Ono, Algebraic solitary waves in stratified fluid. *J. Phys. Soc. Japan* 39 (1975) 1082–1091.
4. T. Kubota, D. R. S. Ko and L. D. Dobbs, Weakly-nonlinear, long internal gravity waves in stratified fluids of finite depth. *J. Hydronautics* 12 (1978) 157–165.
5. H. Segur and J. L. Hammack, Soliton models of long internal waves. *J. Fluid Mech.* 118 (1982) 285–304.
6. J. N. Hunt, Interfacial waves of finite amplitude. *La Houille Blanche* 16 (1961) 515–525.
7. G. H. Keulegen, Characteristics of internal solitary waves. *J. Res. N.B.S.* 51 (1953) 133–140.
8. M. M. Rienecker and J. D. Fenton, A Fourier approximation method for steady water waves. *J. Fluid Mech.* 104 (1981) 119–137.
9. D. Scullen and E. O. Tuck, Nonlinear free-surface flow computations for submerged cylinders. *J. Ship Research* 39 (1995) 185–193.

10. J. M. Vanden-Broeck and L. W. Schwartz, Numerical computation of steep gravity waves in shallow water. *J. Phys. Fluids* 22 (1979) 1868–1871.
11. G. G. Stokes, On the theory of oscillatory waves. *Mathematical and Physical Papers* 1 (1847) 197–229.
12. L. W. Schwartz, Computer extension and analytic continuation of Stokes' expansion for gravity waves. *J. Fluid Mech.* 62 (1974) 553–578.
13. E. D. Cokelet, Steep gravity waves in water of arbitrary uniform depth. *Philos. Trans. R. Soc. London Ser. A* 286 (1977) 183–230.
14. M. S. Longuet-Higgins, Integral properties of periodic gravity waves of finite amplitude. *Proc. R. Soc. London Ser. A* 342 (1975) 157–174.
15. J. Y. Holyer, Large amplitude progressive interfacial waves. *J. Fluid Mech.* 93 (1979) 433–448.
16. P. G. Saffman and H. C. Yuen, Finite-amplitude interfacial waves in the presence of a current. *J. Fluid Mech.* 123 (1982) 459–476.
17. J. M. Vanden-Broeck, Numerical calculation of gravity-capillary interfacial waves of finite amplitude. *J. Phys. Fluids* 23 (1980) 1723–1726.
18. J. H. Michell, The highest waves in water. *Philos. Mag.* 36 (1893) 430–437.
19. J. N. Newman, *Marine Hydrodynamics.* Cambridge (U.S.A.): MIT Press, (1977) 161pp.